Efficient Adsorption of Pb(II) by Sodium Dodecyl Benzene Sulfonate Intercalated Calcium Aluminum Hydrotalcites: Kinetic, Isotherm and Mechanisms

Rongying Zeng (zengry13@163.com)
Hengyang Normal University
Wenqing Tang
Hengyang Normal University
Qianyi Zhou
Hengyang Normal University
Xing Liu
Hengyang Normal University
Yan Liu
Hengyang Normal University
Shuzhan Wang
Hengyang Normal University
Zhen Chen
Hengyang Normal University
Nengzhong Yi
Hengyang Normal University
Zefen Wang
Hengyang Normal University
Jun Chen
Hengyang Normal University

Research Article

Keywords: CaAl-LDHs, SDBS-CaAl-LDHs, Lead ion, Adsorption isotherm, Adsorption mechanism

Posted Date: November 30th, 2021

DOI: https://doi.org/10.21203/rs.3.rs-1036680/v1

Version of Record: A version of this preprint was published at Environmental Science and Pollution Research on February 14th, 2022. See the published version at https://doi.org/10.1007/s11356-022-19129-7.

Abstract

CaAl-LDHs and sodium dodecyl benzene sulfonate (SDBS) intercalated CaAl-LDHs (SDBS-CaAl-LDHs) was acquired by co-precipitation. The two samples were characterized by XRD, XPS, FT-IR, TG and SEM. The factors affecting adsorption (pH, adsorption time，initial concentration) of Pb^{2+} by two adsorbents were studied. The results showed that SDBS-CaAl-LDHs has higher adsorption ability for lead ions removal than that of CaAl-LDHs. Kinetic data for lead ions were in keeping with pseudo-2nd-order model, the adsorption isotherms followed Langmuir and Freundlich isotherm model for CaAl-LDHs. The adsorption by SDBS-CaAl-LDHs were in keeping with the pseudo-second-order kinetic and Langmuir model, suggesting lead ions were chemical adsorption. Adsorption was thought to *form* through Pb species in the precipitates, such as formation of hydroxides and carbonates for lead ions by XRD analysis. Therefore, based on the structural and morphological features, as well as XRD, XPS and SEM, the lead ion adsorption mechanism on SDBS-CaAl-LDHs involved the electrostatic attraction, precipitation, complexation and ion exchange. The Langmuir adsorption capacities for SDBS-CaAl-LDHs were found as 797.63, 828.76, 854.29 $mg \times g^{-1}$ at 293k, 303k, 313k, respectively, when the pH is about 5.2, and thus, making it a highly economical adsorbent for the treatment of contaminated water.

1. Introduction

Lead ion in the aquatic environment arouse serious threat to human health because of their bioaccumulation, toxicity, and potential biomagnifications (Kumar et al. 2017). The Pb(II) maximum concentration of central drinking water in the environmental quality shandards for surface water (GB 3838-2002) is ≤ 0.05 mg/L, while the maximum discharge concentration of Pb(II) for industrial effluents in the integrated wastewater discharge standard (GB8978-1996) is 1.0 mg/L in China, respectively. Therefore, the removal Pb(II) from wastewater is important to mitigate the heavy metal risk of affecting the environment and human health by the various technologies.

The common technologies for Pb(II) removal have included adsorption (Tian et al. 2020), chemical precipitation (Chen et al. 2018), electrolysis (Tao et al. 2014), ion exchange, membrane separation (Berbar et al. 2019), phytoremediation (Wang et al. 2018), biological flocculation and so on. Adsorption method is considered a suitable techniques for wastewater treatment because it has simple design, good adsorption efficiency and low cost for heavy metals. Adsorption of Pb(II) using cost-efficient adsorbents has been studied in the last few years, such as bentonite (Niu et al. 2020), activated carbon (Liu et al. 2019), fly ash (Huang et al. 2020), clay (Abukhadra et al. 2019), zeolite (Han et al. 2020) and so on. These adsorbents have a slow adsorption kinetics and low adsorption capacities for adsorbing heavy metal ions from wastewater (Gupta et al. 2010). Thus, finding a high application potential for adsorbent with relatively good adsorption capability has become the hot topic of the research.

Layered double hydroxides (LDHs) are considered to be a class of anion clay with layered structure. Their general formula are $[M^{2+}_{1-x} M^{3+}_{x} (OH)_2]^{x+}[A^{n-}_{x/n}]\cdot yH_2O$, where M^{2+} and M^{3+} represent divalent and trivalent metal ion, A^{n-} is an interlayer anion (Grover et al. 2019). Because of its ion-exchange ability,

adjustable element proportions, special-layered structure and operation of simple synthesis, LDHs and modified materials of LDHs were widely studied in wastewater treatment. For example, Yang et al (Yang et al. 2016) used Mg–Al layered double hydroxides modified palygorskite (Pal/MgAl-LDH) as adsorbent to remove Pb^{2+}, Cu^{2+}, Ni^{2+} with the maximum adsorption capacity 99.8, 64.0, 41.8 mg g^{-1} at pH 5.0, respectively. Jia et al (Jia et al., 2019) utilized magnetic biochar supporting MgFe-LDH composites to remove Pb^{2+}, found that the maximum adsorption capacity 476.25 mg g^{-1}, the adsorption process mainly contain chemisorptions. Zhu et al (Zhu et al. 2020) studied the removal of Cu^{2+} and Pb^{2+} by amino trimethylene phosphonic acid (ATMP) Intercalated Zn-Al layered double hydroxide, and the adsorption capacity for Cu^{2+} and Pb^{2+} were 42.02 and 84.06 mg g^{-1}.

The homogeneous dispersion of LDHs is a technical challenge because the layered surface of LDHs contains a large number of active hydroxyl groups. To improve dispersion of LDHs, a possible solution is transforming the hydrophilic LDHs into hydrophobic one by surfactant-intercalated LDHs such as sodium dodecyl sulfate (SDS) (Ahmed et al. 2015; Zhang et al. 2012), Sodium Dodecyl Benzene Sulfate (SDBS) (Zhang et al. 2014), sodium hexadecyl sulfate (SHS) (Zhang et al. 2015) into LDHs, interlayer spaces. In the literature, the synthesis of surfactant-intercalated LDHs had been extensively used to remove organic contaminants such as pesticides (Bruna et al. 2006), herbicides (Carrizosa et al. 2004), dyes (Zhang et al. 2017; Zhu et al. 2020), phenols (Zaghouane-boudiaf et al. 2011). However, to the best of our knowledge, the removal of heavy metal ions from aqueous solutions were not reported elsewhere by surfactant-intercalated Ca-Al layered double hydroxides (CaAl-LDHs).

In the present work, we describe the preparation of SDBS-intercalated CaAl-LDHs (SDBS-CaAl-LDHs), and the study of the lead ions removal process for wastewaters, and its adsorption effect is compared to that of CaAl-LDHs used as sorbent.

2. Experimental Section

2.1 CaAl-LDHs preparation

The CaAl-LDHs with a Ca:Al ratio of 3:1 was synthesized by co-precipitation, according to the method described by Wang and Grover (Grover et al. 2019; Wang et al. 2020). In brief, first, CaO, $Al(NO_3)_3{\cdot}9H_2O$ and urea were separately dispersed in deionized water with ultrasonication for 0.5 h, next $Al(NO_3)_3$ and urea solution were added to the suspension of $Ca(OH)_2$ drop by drop while refluxing at 100 ℃ on a magnetic stirrer. After that, this slurry was filtered, washed, dried, and ground into powder (mesh size is 30), namely CaAl-LDHs.

2.2 SDBS-CaAl-LDHs preparation

CaAl-LDHs power was calcined at 400 ℃ for 2 h to obtain layered double oxides (CaAl-LDO). 2.8g CaAl-LDO was added to 5.8 g SDBS solution at room temperature under magnetic stirring, and transferred into

autoclave at 150 °C for 1.5 h. After, the sample was filtrated and washed at normal temperature, dried at 60 °C in an oven. The finished product of SDBS-CaAl-LDHs is finally obtained by sieving.

2.3 Batch sorption experiments

Adsorption capacity and removal rate are the main factors to investigate the adsorption performance for adsorbent. In this study, in order to estimate the adsorption capacity and removal rate of adsorbent, constant amount of SDBS-CaAl-LDHs and CaAl-LDHs were added to Pb^{2+} aqueous solutions. The mixture was shaken by the thermostated shaker for a sufficient time at a specified temperature. To reach adsorption equilibrium, the suspensions was easily separated and the lead ion concentration residue was tested. Adsorption capacity and removal rate of lead ions can be estimated using equation (1) ~ (3).

$$Q_e = (C_0 - C_e)V / m \quad (1)$$

$$Q_t = (C_0 - C_t)V / m \quad (2)$$

$$R\% = 100\% \times (C_0 - C_e) / C_0 \quad (3)$$

where, Q_e and Q_t (mg g^{-1}) are the adsorption capacity of lead ions adsorbed at equibrium time and time t; C_0, C_e and C_t (mg L^{-1}) are the lead ion concentration at the initial time, equilibrium time and time t, respectively; m (g) is the weight of adsorbent; V (L) is the volume of lead ion solution; R% is removal rate.

2.4 Characterization

The characteristics of SDBS-CaAl-LDHs and CaAl-LDHs, the mechanisms for adsorbing Pb^{2+} were inspected by SEM (Sigma HD), XRD (X' Pert PRO), FT-IR (Shimadzu Corporation, Japan), and XPS (Thermo Scientific K-Alpha+). The thermal stability of CaAl-LDHs and SDBS-CaAl-LDHs were characterized using 209F3 thermal analyzer.

3 Results And Discussion

3.1 General characterization

The FT-IR spectrum of CaAl-LDHs and SDBS-CaAl-LDHs were investigated in Fig. 1. A peak at 3400-3700 cm^{-1} and a weak peak at 1625 cm^{-1} were related to the –OH stretching and bending vibrations of the metal hydroxide layers and interlayer water molecules, a peaks at 1381 cm^{-1} was ascribed to the NO_3^- ions stretching vibration (Gupta et al. 2020). A very strong peak at 1355 cm^{-1} and 1407 cm^{-1}represent CO_3^{2-} stretching mode (Jia et al. 2019). Several peaks observed in 1000–400 cm^{-1} mainly belonged to characteristic peaks of Ca-O and Al-O bonds (Sun et al. 2017). Two bands located at 2982 and 2873 cm^{-1} were due to the C-H stretching vibration bands of dodecylsulfate ions in SDBS-CaAl-LDHs (b). The sulfate S=O stretch at 1187 and 1066 cm^{-1} were also observed (Bouraada et al. 2008).

The decomposition temperatures and mass loss of CaAl-LDHs and SDBS-CaAl-LDHs have been performed by the TG-DTG analysis (Fig. 2). The TG-DTG curve of CaAl-LDHs (Fig. 2 (a)) showed the major mass loss stages. The initial weight loss of 8.21% before 165 °C (step 1) was due to the loss of surface adsorbed water and step 2 at 165-425°C, bigger than step 1 (weight loss of 16.24% for step 2), to the loss of interlayer water; weight loss of 17.45% in three step above 425 °C is lattice water, the decomposition of CO_3^{2-} and dehydroxylation from CaAl-LDHs layers. The total weight loss for CaAl-LDHs was 41.90%. Compared with the curve of CaAl-LDHs (Fig. 2 (a)), the TG-DTG curve of SDBS-CaAl-LDHs (Fig. 2 (b)) showed two major mass loss stages. The initial weight loss of 11.80% before 540 °C was due to the loss of adsorbed water, lattice water, and the decomposition of the intercalated SDBS and CO_3^{2-} from LDHs of SDBS-CaAl-LDHs (Sun et al. 2017; Mahioubi et al. 2019). The weight loss of 29.22% from 540 to 800 °C in the second step corresponded to the dehydroxylation of SDBS-CaAl-LDHs layers (Sun et al. 2017). The total weight loss for SDBS-CaAl-LDHs was 40.02%. Therefore, the residue amount in the CaAl-LDHs was much lower than that of SDBS-CaAl-LDHs material.

3.2 Adsorption isotherms

Adsorption isotherms are useful to provide qualitative information on equilibrium adsorption capacity of CaAl-LDHs and SDBS-CaAl-LDHs and equilibrium concentration of lead ions between the solid and liquid phase. Herein, equilibrium adsorption isotherms, such as Langmuir and Freundlich, were applied to represent the adsorption data of lead ions on CaAl-LDHs and SDBS-CaAl-LDHs powders. They were given in Eqs. (4-5) (Langmuir et al. 1918; Freundlich et al. 1907).

$$Q_e = K_L Q_m C_e / (1 + K_L C_e) \quad (4)$$

$$Q_e = K_f C_e^n \quad (5)$$

where Q_m (mg g^{-1}) and K_L (L mg^{-1}) denote the maximum adsorption capacity related to the complete monolayer coverage of CaAl-LDHs and SDBS-CaAl-LDHs and the Langmuir adsorption equilibrium constant corresponding to the adsorption energy. K_f (mg^{1-n} L^n g^{-1}) and n (dimensionless constant) are Freundlich constant corresponding to the adsorption capacity and adsorption intensity, respctively. If the values of n is between 0 and 1, which indicate a favorable adsorption (Zeng et al. 2018; Zeng et al. 2019).

The removal rate, Freundlich and Langmuir isotherms for different initial Pb^{2+} concentration adsorption on the synthesized CaAl-LDHs and SDBS-CaAl-LDHs are shown in Fig. 3(a)~(h). As shown in Fig. 3(a)~(d), the removal rate (R%) of CaAl-LDHs and SDBS-CaAl-LDHs reduces gradually with rising Pb^{2+} concentration, however, the sorption capacity (Q_e) exactly the opposite at three temperature. The Pb^{2+} removal rate (R%) by CaAl-LDHs was lower than that by SDBS-CaAl-LDHs at the same dosage. Such as the dosage is 0.5 g L^{-1}, the Pb^{2+} removal rate of CaAl-LDHs and SDBS-CaAl-LDHs are 87.11% and 98.84% as 300 mg $L^{-1}$for Pb^{2+} initial concentration at 303 K. In addition, Q_e of CaAl-LDHs and SDBS-CaAl-LDHs increase when increasing the initial concentration of

Pb^{2+} and Q_e increase more swiftly at low concentration of Pb^{2+}. This shows that a lot of lead ions are deposited on the surface of adsorbent with the increase of Pb^{2+} concentration. From the experimental data, Q_e of SDBS-CaAl-LDHs in 303 K is 681.5 mg g^{-1} (C_0=350 mg L^{-1}, m=0.05 g) which is 1.494 times higher than Q_e (456.15 mg g^{-1}) of CaAl-LDHs (C_0=300mg L^{-1}, m=0.06g). It also shows that CaAl-LDHs intercalated with surfactant to improve the adsorption capacity is a significant modification method.

Fig. 3(e)~(h) are Freundlich and Langmuir isotherms. Table 1 presents the constants (Q_m, K_L; K_f, n) and correlation coefficients (R^2) of Langmuir and Freundlich isotherm models of CaAl-LDHs and SDBS-CaAl-LDHs for the adsorption of Pb^{2+}. The result exposes that the adsorption data of lead ions on CaAl-LDHs were fitting well with the Langmuir and Freundlich model, the correlation coefficient R^2 of Langmuir and Freundlich model are 0.9689, 0.9746, 0.9764 and 0.9723, 0.9827, 0.9776 at three temperatures, respectively. The experimental data of lead ions on SDBS-CaAl-LDHs indicates the Langmuir model has highly fitting than the Freundlich model, the correlation coefficient R^2 of Langmuir model are 0.9852, 0.9845, 0.9899 at three temperatures, respectively. The Langmuir adsorption capacities (Q_m) for CaAl-LDHs and SDBS-CaAl-LDHs were found as 717.17, 815.07, 782.51 and 797.63, 828.76, 854.29 mg×g^{-1}, respectively. The K_L value of SDBS-CaAl-LDHs is significantly higher than that of CaAl-LDHs, suggesting that SDBS-CaAl-LDHs has strong adsorption ability (Jia et al. 2019). The value of n for two materials are below 1, the lowerer value of n of SDBS-CaAl-LDHs than that of CaAl-LDHs suggests that SDBS-CaAl-LDHs has better adsorption performance.

Q_m of Pb^{2+} ions for SDBS-CaAl-LDHs and CaAl-LDHs was compared to the other adsorbents in previous studies (Hou et al. 2020; Dinari et al. 2020; Zhao et al. 2011) and the result is listed in Table 2. It is clearly that SDBS-CaAl-LDHs has a better adsorption capacity than other materials.

3.3 Adsorption Kinetics

The contact time, as one of the important factor for the analysis of lead removal on adsorbent (SDBS-CaAl-LDH, CaAl-LDH), was studied (Fig. 4). The results showed that removal rate (R%) (Fig. 4(a), (b)) and adsorption capacity (Q_t) on adsorption of Pb(II) to adsorbent was rapidly growing in initial 30 min, then slowly increasing from 30 min to 60 min and remaining unchanged later. The results could be proposed for the removal mechanism: due to countless adsorption sites at the initial stage, which can be available for the fast Pb(II) sorption process from the solution to the external surfaces of adsorbents (SDBS-CaAl-LDH, CaAl-LDH), this sorption process was considered to the rapid diffusion of lead ions ; then slow sorption was owed to slow diffusion of lead ions from boundary layer to interlayer space of adsorbent and replacing Ca(II) by Pb(II) on the interlayer surface of SDBS-CaAl-LDH or CaAl-LDH as reported (Chen et al. 2016), So sorption curves increase slowly by slow diffusion at a later stage. As time proceeds, lead ions diffused into the porous structure of SDBS-CaAl-LDH or CaAl-LDH leading to little variation for sorption curves.

Rapid adsorption is very useful criterion for identifying adsorption efficiency of adsorbent. Generally, two different models (the pseudo-first-order and pseudo-second-order models) are served to investigate the kinetic behavior of lead ions on CaAl-LDHs and SDBS-CaAl-LDHs , two kinetics equation can be shown below (Zeng et al. 2018; Zeng et al. 2019):

$$Q_t = Q_e(1 - \exp(-K_1 t)) \qquad (6)$$

$$Q_t = (tK_2Q_e^2) / (1 + tK_2Q_e) \qquad (7)$$

where K_1 (min^{-1}) and K_2 (g mg^{-1} min^{-1}) represent rate constants for pseudo 1st order and pseudo 2nd order models, respectively.

In order to complete lead ions removal by two adsorbents, adsorption kinetic curves in Fig.4(c)~(f) were fitted and the kinetic model corresponding parameters were obtained in Table 3. Calculated sorption capacity ($Q_{e,cal}$) for CaAl-LDHs and SDBS-CaAl-LDHs in pseudo 2nd order models were found as 460.41, 466.76, 471.47 and 699.43, 710.22, 714.19 mg×g^{-1}at 293, 303, 313 K, respectively. $Q_{e,cal}$ for CaAl-LDHs and SDBS-CaAl-LDHs in pseudo 1st order models were found as 446.91, 454.06, 458.78 and 660.00, 674.36, 679.77 mg×g^{-1}at 293, 303, 313 K, respectively. Experimental sorption capacity ($Q_{e,exp}$) for CaAl-LDHs and SDBS-CaAl-LDHs were found as 457.32, 464.85, 470.70 and 681.26, 685.70, 692.90 mg×g^{-1} at 293, 303, 313 K, respectively. Sorption capacity are contrasted with the value of $Q_{e,cal}$ by pseudo 1st order and pseudo 2nd order models and $Q_{e,exp}$, $Q_{e,cal}$ for pseudo 2nd order models was close to $Q_{e,exp}$. In addition, the correlation coefficient R^2 (R^2 = 0.970~0.999) of two adsorbents for pseudo 2nd order models were more than that of pseudo 1st order model (R^2 =0.842~0.954), respectively. The results showed that pseudo 2nd order model is more suitable than pseudo 1st order model to describe the sorption of lead ions on CaAl-LDHs and SDBS-CaAl-LDHs, predicting that the chemisorption is a rate-limited process (Zhang et al. 2017).

3.4 Effect of pH on sorption of Pb^{2+}

Effect of pH during sorption of Pb^{2+} on the CaAl-LDHs and SDBS-CaAl-LDHs were studied and results were listed in Fig. 5. showed that lead may form precipitation of $Pb(OH)_2$ at pH greater than 8 in the previuos literature (Zeng et al. 2019), So the pH values in this study were studied from 2.0 to 7.0, respectively, and the results were listed in Fig. 5. The adsorption capacity (Q_e) and removal rate (R%) of CaAl-LDHs and SDBS-CaAl-LDHs for Pb^{2+} increased significantly as pH between 2.0 and 5.0, and Q_e and R% of two adsorbents increased slowly as pH between 5.0 and 7.0, Q_e and R% of SDBS-CaAl-LDHs was higher than that of CaAl-LDHs. Leads ion sorption got to equilibrium at pH of about 5 (*the solution pH*), adsorption capacities of CaAl-LDHs and SDBS-CaAl-LDHs were achieved 456 mg/g (the dosage of 0.6 g L^{-1}) and 678 mg/g (the dosage of 0.5 g L-1) at 303 K, respectively. Therefore, SDBS-CaAl-LDHs exhibit the highest activity of lead ions adsorption in solution. Q_e and R% were low at low p*H*, it may be

due to the fact that hydrogen ions took up the available binding sites of CaAl-LDHs and SDBS-CaAl-LDHs. Similar result was obtained in the literature (Hou et al. 2020).

3.5 Adsorption mechanisms

Adsorption of lead ions on CaAl-LDHs and SDBS-CaAl-LDHs might come up by three paths (i) external surface adsorption of lead ions by electrostatic interactions and complexation, (ii) replacement of interlayer calcium ions by cation exchange, (iii) formation of Pb precipitates.

XRD patterns of CaAl-LDHs and SDBS-CaAl-LDHs before and after lead ions adsorption were shown in Fig. 6. The diffraction peak positions of CaAl-LDHs and SDBS-CaAl-LDHs could be compared with the pure hexagonal phase recorded on PDF 78-1219 (Zhang et al. 2012). The diffraction peak positions of CaAl-LDHs (a) and SDBS-CaAl-LDHs (c) have a slight deviation, peak were discovered at about 10° (002), 21°(004), 30°(006), 56° (110). Sharp peaks at around 30° may also be attributed to Calcium carbonate(JCPDS 17-863). Peak intensity for SDBS-CaAl-LDHs in (002) and (004) were higher than that of CaAl-LDHs. After Pb^{2+} ions adsorption (Fig. 6 (b), (d)), the XRD diffraction peak find the new phase lead hydroxide nitrate ($Pb_3(OH)_5NO_3$, JCPDS 22-0659) (Rojas et al. 2014) and $Pb_3(CO_3)_2(OH)_2$ (JCPDS 13-013) (Jia et al. 2019) from surface co-precipitation between Pb^{2+} and interlayer CO_3^{2-} , surface hydroxyl groups of CaAl-LDHs and SDBS-CaAl-LDHs. This might be related to dissolution-precipitation mechanism of Ca Al layered double hydroxides in the solution (Zhang et al. 2012; Rojas et al. 2014).

The SEM images of CaAl-LDHs and SDBS-CaAl-LDHs before and after lead ions adsorption are shown in Fig.7. CaAl-LDHs (a) was formed from the approximately hexagonal platy crystallites. Compared with CaAl-LDHs (Fig.7 (a)), the resulting solid of SDBS-CaAl-LDHs (Fig.7 (c)) discovered obvious changes in image, which agglomerated plate-shaped particles were observed. SDBS-CaAl-LDHs showed somehow irregular shapes because of some aggregations. The result showed that the morphology of LDHs can be influenced in presence of large organic anions. The SEM after adsorption (Fig. 7(b), (d)) showed that CaAl-LDHs and SDBS-CaAl-LDHs surface adsorb lead ions by forming Pb precipitates. The layered structure of particle plates for CaAl-LDHs and SDBS-CaAl-LDHs changed, which was just identical with the XRD results.

The elemental compositions of CaAl-LDHs and SDBS-CaAl-LDHs before and after lead ions adsorption were studied by XPS spectrum (Fig. 8). As shown in Fig. 8(a), CaAl-LDHs were not only the predominant elements of O, N, Ca, Al but also C element from pore expanding agent of urea. Compared with CaAl-LDHs, SDBS-CaAl-LDHs (Fig. 8(a)) discovered S element, which demonstrate that the SDBS is intercalated into CaAl-LDHs.

In this research, to identify the changed chemical environment of CaAl-LDHs and SDBS-CaAl-LDHs before and after lead ions adsorption, some complementary XPS experiments (Al, Ca, O, Pb elements) were checked as shown in Fig. 8(b)~(d). As may be seen from Fig. 8(b), the binding energy of Ca 2p has two

peaks at around 346 and 350 eV (346.98 and 350.38 eV for CaAl-LDHs, 346.98 and 350.48 eV for CaAl-LDHs-Pb, 346.78 and 350.28 eV for SDBS-CaAl-LDHs, 346.68 and 350.18 eV for SDBS-CaAl-LDHs-Pb). Compared with the binding energy of Ca 2p for CaAl-LDHs and SDBS-CaAl-LDHs before and after lead ions adsorption, the results showed that two peaks of Ca 2p from SDBS-CaAl-LDHs had change whereas a peak from CaAl-LDHs had change. The binding energies of Al 2p for CaAl-LDHs and SDBS-CaAl-LDHs Fig. 8(c) were 73.98 and 73.88 eV, respectively , decreasing with 0.1 eV for SDBS-CaAl-LDHs. However, compared with the binding energy of Al 2p after sorption Pb(II) ion, shifts in binding energy(reduction of 0.1 eV for CaAl-LDHs and increase of 0.1 eV for SDBS-CaAl-LDHs) were observed. Two XPS peaks for CaAl-LDHs (138.28 and 143.18 eV) and SDBS-CaAl-LDHs (138.58 and 143.58 eV) after sorption Pb(II) ion (Fig. 8(a), (d)) were observed which resulted from Pb 4f absorption. This result shows the existence of both Pb species in the precipitates, such as formation of hydroxides and carbonates for lead ions. The XPS result is in agreement with the XRD result (Fig.6). This result also shows that the main reactions in the lead ions removal by SDBS-CaAl-LDHs and CaAl-LDHs are precipitation and surface adsorption, are consistent with the literature report (Park et al. 2007). These slight shifts in binding energies prove the dominance of complexation mechanism (Gupta et al. 2020) Thus, SDBS-CaAl-LDHs or CaAl-LDHs formed complex with lead ions through specific adsorption (such as surface complexation) and nonspecific adsorption (such as electrostatic interactions including cation exchange) as described in equation (8-9) (Li et al. 2017) and Fig. 9.

$$\text{Sur-OH} + Pb^{2+} \rightarrow \text{Sur-O-}Pb^{+} + H^{+} \quad \text{specific adsorption} \quad (8)$$

$$\text{Sur-OH} + Pb^{2+} \rightarrow \text{Sur-O}\ldots Pb^{2+} + H^{+} \quad \text{nonspecific adsorption} \quad (9)$$

4. Conclusions

CaAl-LDHs and SDBS intercalated CaAl-LDHs were prepared by a effective, environment friendly and facile method because water is the only solvent used. SDBS-CaAl-LDHs has strong adsorption ability for refining Pb^{2+} than that of CaAl-LDHs. The adsorption of lead ions by CaAl-LDHs and SDBS-CaAl-LDHs were in keeping with the pseudo-second-order kinetic and Langmuir model, which showed chemical adsorption. Adsorption was thought to *form* through Pb species in the precipitates, such as formation of hydroxides and carbonates for lead ions by XRD analysis. The Langmuir adsorption capacities for CaAl-LDHs and SDBS-CaAl-LDHs were found as 717.17, 815.07, 782.51 and 797.63, 828.76, 854.29 $mg \times g^{-1}$, respectively, when the pH is about 5.2.

Declarations

Funding

This study is supported by the Natural Science Foundation of Hunan Province (No.2021JJ50021); The Scientific Research Project of Hengyang Normal University (No.19QD16; No.2020QD08; NYD202026); The Scientific Research Project of Ecology and Environment Department of Hunan (No.2020-29);

National Training Program of Innovation and Entrepreneurship for Undergraduate (No. S201910546002X) and Training Program of Innovation and Entrepreneurship for Undergraduate of Hunan Province (No. cxcy2027: S202010546027S; No. cxcy2021025: S202110546010X)

Author information

Affiliations

Hunan Engineering Research Center for Monitoring and Treatment of Heavy Metal Pollution in the Upper Reaches of Xiangjiang River, Key Laboratory of Functional Organometallic Materials of College of Hunan Province, College of Chemistry and Material Science, Hengyang Normal University, Hengyang, 421001, PR China.

Rongying Zeng, Wenqing Tang, Xing Liu, Qianyi Zhou, Yan Liu, Shuzhan Wang, Zhen Chen, Nengzhong Yi, Zefen Wang

Changde Xinfurong Environmental Protection Co., Ltd.

Jun Chen

Contributions

All authors contributed to the study conception and design. Material preparation, data collection, and analysis were performed by Qianyi Zhou, Yan Liu, Shuzhan Wang, Zhen Chen and Nengzhong Yi. Material characterization and sorption kinetic data analysis were performed by Xing Liu and Zefen Wang. The first draft of the manuscript was written by Rongying Zeng and Wenqing Tang. And all authors commented on previous versions of the manuscript. All authors read and approved the final manuscript.

Corresponding authors

Correspondence to Wenqing Tang

Ethics approval and consent to participate

Not applicable.

Consent for publication

Not applicable.

Conflict of interest

The authors declare that they have no conflict of interest.

Availability of data and materials

Not applicable.

References

Abukhadra MR, Bakry BM, Adlii A, Yakout SM, El-Zaidy ME (2019) Facile conversion of kaolinite into clay nanotubes (KNTs) of enhanced adsorption properties for toxic heavy metals (Zn^{2+}, Cd^{2+}, Pb^{2+}, and Cr^{6+}) from water. J Hazard Mat 374:296-308

Ahmed AAA, Talib ZA, Hussein MZ (2015) Influence of sodium dodecyl sulfate concentration on the photocatalytic activity and dielectric properties of intercalated sodium dodecyl sulfate into Zn-Cd-Al layered double hydroxide. Mater Res Bull 62:122-131

Berbar Y, Hammache ZE, Bensaadi S, Soukeur R, Amara M, Bruggen BV (2019) Effect of functionalized silica nanoparticles on sulfonated polyethersulfone ion exchange membrane for removal of lead and cadmium ions from aqueous solutions. J Water Process Eng 32:100953

Bouraada M, Lafjah M, Ouali MS, De Menorval LC (2008) Basic dye removal from aqueous solutions by dodecylsulfate- and dodecyl benzene sulfonate-intercalated hydrotalcite. J Hazard Mater 153:911-918

Bruna F, Pavlovic I, Barriga C, Cornejo J, Ulibarri MA (2006) Adsorption of pesticides carbetamide and metamitron on organohydrotalcite. Appl Clay Sci 33: 116-124

Carrizosa MJ, Koskinen WC, Hermosin MC (2004) Interactions of acidic herbicides bentazon and dicamba with organoclays. Soil Sci Soc Am J 68:1863-1866

Chen H, Qian G, Ruan X, Frost RL (2016) Removal process of nickel(II) by using dodecyl sulfate intercalated calcium aluminum layered double hydroxide. Appl. Clay Sci. 132-133, 419-424.

Chen Q, Yao Y, Li X, Lu J, Zhou J, Huang Z (2018) Comparison of heavy metal removals from aqueous solutions by chemical precipitation and characteristics of precipitates. J Water Process Eng 26:289-300

Dinari M, Neamati S (2020) Surface modified layered double hydroxide/ polyaniline nanocomposites: Synthesis, characterization and Pb^{2+} removal. Colloid Surface A 589:124438

Freundlich H (1907) Udber die adsorption in Loesunger. Z Physik Chem 57:385-470

Grover A, Mohiuddin I, Malik AK, Aulakh JS, Kim KH (2019) Zn-Al layered double hydroxides intercalated with surfactant: Synthesis and applications for efficient removal of organic dyes. J Clean Prod 240:118090

Gupta VK, Rastogi A, Nayak A (2010) Adsorption studies on the removal of hexavalent chromium from aqueous solution using a low cost fertilizer industry waste material. J Colloid Interface Sci 342:135-141

Gupta NK, Saifuddin M, Kim S, Kim KS (2020) Microscopic, spectroscopic, and experimental approach towards understanding the phosphate adsorption onto Zn-Fe layered double hydroxide. J Mol Liq 297:111935

Han L, Wang J, Liu Z, Zhang Y, Jin Y, Li J, Wang D (2020) Synthesis of fly ash-based self-supported zeolites foam geopolymer *via* saturated steam treatment. J Hazard Mat 393:122468

Hou T, Yan L, Li J, Yang Y, Shan L, Meng X, Li X, Zhao Y (2020) Adsorption performance and mechanistic study of heavy metals by facile synthesized magnetic layered double oxide/carbon composite from spent adsorbent. Chem Eng J 384:123331

Huang X, Zhao H, Zhang G, Li J, Yang Y, Ji P (2020) Potential of removing Cd(II) and Pb(II) from contaminated water using a newly modified fly ash. Chemosphere 242:125148

Jia Y, Zhang Y, Fu J, Yuan L, Li Z, Liu C, Zhao D, Wang X (2019) A novel magnetic biochar/MgFe-layered double hydroxides composite removing Pb^{2+} from aqueous solution: Isotherms, kinetics and thermodynamics. Colloids Surf A 567: 278-287

Kumar R, Sharma RK, Singh AP (2017) Cellulose based grafted biosorbents- Journey from lignocellulose biomass to toxic metal ions sorption applications-A review. J Mol Liq 232:62-93

Langmuir I (1918) The adsorption of gases on plane surfaces of glass, mica and Platnum. J Am Chem Soc 40:1361-1403

Li SS, Jiang M, Jiang TJ, Liu JH, Guo Z, Huang XJ (2017) Competitive adsorption behavior toward metal ions on nano-Fe/Mg/Ni ternary layered double hydroxide proved by XPS: Evidence of selective and sensitive detection of Pb(II), J. Hazard. Mat. (2017) 1-10.

Liu X, Lai D, Wang Y (2019) Performance of Pb(II) removal by an active carbon supported nanoscale zero-valent iron composite at ultralow iron content. J Hazard Mat 361:37-48

Mahjoubi FZ, Khalidi A, Elhalil A, Barka N (2019) Characteristics and mechanisms of methyl orange sorption onto Zn/Al layered double hydroxide intercalated by dodecyl sulfate anion. Scientific African 6:1-11

Niu M, Li G, Cao L, Wang X, Wang W (2020) Preparation of sulphate aluminate cement amended *bentonite* and its use in heavy metal adsorption. J Clean Prod 256:120700.

Park M, Choi CL, Seo YJ, Yeo SK, Choi J, Komarneni S, Lee JH (2007) Reactions of Cu^{2+} and Pb^{2+} with Mg/Al layered double hydroxide. Appl Clay Sci 37:143-148

Rojas R (2014) Copper, lead and cadmium removal by Ca Al layered double hydroxides. Appl Clay Sci 87:254-259

Sun M, Zhang P, Wu D, Frost RL (2017) Novel approach to fabricate organo-LDH hybrid by the intercalation of sodium hexadecyl sulfate into tricalcium aluminate. Appl Clay Sci 140:25-30

Tao HC, Lei T, Shi G, Sun XN, Wei XY, Zhang LJ, Wu WM (2014) Removal of heavy metals from fly ash leachate using combined bioelectrochemical systems and electrolysis. J Hazard Mat 264:1-7

Tian Y, Li J, Whitcombe TW, McGill WB, Thring R (2020) Application of oily sludge-derived char for lead and cadmium removal from aqueous solution. Chem Eng J 384:123386

Wang L, Lin H, Dong Y, He Y (2018) Effects of cropping patterns of four plants on the phytoremediation of vanadium-containing synthetic wastewater. Ecol Eng 115:27-34

Wang H, Wang S, Chen Z, Zhou X, Wang J, Chen Z (2020) Engineered biochar with anisotropic layered double hydroxide nanosheets to simultaneously and efficiently capture Pb^{2+} and CrO_4^{2-} from electroplating wastewater. Bioresource Technol 306:123118

Yang F, Sun S, Chen X, Chang Y, Zha F, Lei Z (2016) Mg-Al layered double hydroxides modified clay adsorbents for efficient removal of Pb^{2+}, Cu^{2+} and Ni^{2+} from water. Appl Clay Sci 123:134-140

Zaghouane-boudiaf H, Boutahala M, Tiar C, Arab L, Garin F (2011) Treatment of 2,4,5-trichlorophenol by MgAl-SDBS organo-layered double hydroxides: Kinetic and equilibrium studies. Chem Eng J 173:36-41

Zeng RY, Tang WQ, Ding CX, Yang LH, Gong DX, Kang Z, He ZM, Wu YM (2019) Preparation of anionic-cationic co-substituted hydroxyapatite for heavy metal removal: Performance and mechanisms. J Solid State Chem 280:5-14

Zeng RY, Tang WQ, Liu X, Ding CX, Gong DX (2018) Adsorption of Cu^{2+} from aqueous solutions by Si-substituted carbonate hydroxyapatite prepared from egg-shell: kinetics, isotherms and mechanism studies. Desalin Water Treat 116: 137-147

Zhang D, Zhu MY, Yu JG, Meng HW, Jiao FP (2017) Effective removal of brilliant green from aqueous solution with magnetic Fe_3O_4@SDBS@LDHs composites. Trans. Nonferrous Met Soc China 27:2673-2681

Zhang P, Qian G, Xu ZP, Shi H, Ruan X, Yang J, Frost RL (2012) Effective adsorption of sodium dodecylsulfaten (SDS) by hydrocalumite (CaAl-LDH-Cl) induced by self-dissolution and re-precipitation mechanism. J Colloid Interface Sci 367:264-271

Zhang P, Wang T, Qian G, Frost RL (2014) Organo-LDH synthesized via tricalcium aluminate hydration in the present of Na-dodecylbenzenesulfate aqueous solution and subsequent in vestigated by near-infrared and mid-infrared. Spectrochim Acta A 125:195-200

Zhang P, Wang T, Zhang L, Wu D, Frost RL (2015) XRD, SEM and infrared study into the intercalation of sodium hexadecyl sulfate (SHS) into hydrocalumite. Spectrochim Acta A 151:673-678

Zhao D, Sheng G, Hu J, Chen C, Wang X (2011) The adsorption of Pb(II) on Mg_2Al layered double hydroxide. Chem Eng J 171:167-174

Zhu S, Khan MA, Wang F, Bano Z, Xia M (2020) Rapid Removal of Toxic Metals Cu^{2+} and Pb^{2+} by Amino Trimethylene Phosphonic Acid Intercalated Layered Double Hydroxide: A Combined Experimental and DFT Study. Chem Eng J 392: 123711

Zhu Z, Xiang M, Li P, Shan L, Zhang P (2020) Surfactant-modified three- dimensional layered double hydroxide for the removal of methyl orange and rhodamine B: Extended investigations in binary dye systems. J Solid State Chem 288:121448

Tables

Table 1 Adsorption isotherm parameters for adsorption of Pb^{2+} onto CaAl-LDHs (i) and SDBS-CaAl-LDHs (ii) at different temperature

Equilibrium models	Parameters	Adsorbent	293K	303K	313K
Langmuir	Q_m(mg g^{-1})	i	717.17	815.07	782.51
		ii	797.63	828.76	854.29
	K_L (L g^{-1})	i	0.0547	0.0507	0.0644
		ii	0.2904	0.4968	0.5694
	R^2	i	0.9689	0.9746	0.9764
		ii	0.9852	0.9845	0.9899
Freundlich	K_f(*mg g-1*)	i	101.16	95.95	109.27
		ii	424.99	473.35	495.72
	n	i	0.4131	0.4637	0.4394
		ii	0.1373	0.1329	0.1314
	R^2	i	0.9723	0.9827	0.9776
		ii	0.8970	0.9195	0.8740

Table 2 Comparison of maximum adsorption capacity (Q_m) of Pb^{2+} with other adsorbents

Adsorbent	Q_m (mg g^{-1})	Isotherm	pH	Reference
Mag-LDO/C	359.7	Langmuir	6	(Hou et al. 2020)
ATMP/ Zn-Al LDH	164.84	Langmuir	5.0	(Zhu et al. 2020)
magnetic biochar/MgFe-LDH	476.25	Langmuir	3-6	(Jia et al. 2019)
Mg_2Al–LDH	66.16	Langmuir	7.0	(Zhao et al. 2011)
Pal/MgAl–LDH	281.0	Langmuir	5	(Yang et al. 2016)
PANI/ LDH NCs	109.71	Langmuir and Freundlich	6.0	(Dinari et al. 2020)
CaAl-LDHs	815.07	Langmuir and Freundlich	5.2	This study
SDBS-CaAl-LDHs	854.29	Langmuir	5.2	This study

* Mag-LDO/C : Magnetic layered double oxide/carbon; ATMP/ Zn-Al LDH: Amino Trimethylene Phosphonic Acid Intercalated Layered Double Hydroxide; LS: Sulfonated lignin, LDH: layered double hydroxides; Pal/MgAl-LDH: Mg-Al layered double hydroxides modified palygorskite; PANI/ LDH NCs: Surface modified Ca/Fe layered double hydroxide (LDH) /polyaniline nanocomposites;

Table 3 Kinetic model parameters for adsorption of Pb^{2+} onto CaAl-LDHs (i) and SDBS-CaAl-LDHs (ii) at different temperature

Kinetic models	Parameters	Adsorbent	293K	303K	313K
	$Q_{e,exp}$(mg g^{-1})	i	457.32	464.85	470.70
		ii	681.26	685.70	692.90
Pseudo-first order	$Q_{e,cal}$(mg g^{-1})	i	446.91	454.06	458.78
		ii	660.00	674.36	679.77
	K_1 (min^{-1})	i	0.2979	0.3150	0.3244
		ii	0.1800	0.1941	0.2024
	R^2	i	0.8605	0.8779	0.8421
		ii	0.8812	0.9539	0.9514
Pseudo-second-order	$Q_{e,cal}$(mg g^{-1})	i	460.41	466.76	471.47
		ii	699.43	710.22	714.19
	K_2(×10^{-3} g mg^{-1} min^{-1})	i	1.5085	1.6430	1.6882
		ii	0.4411	0.4933	0.5236
	R^2	i	0.9987	0.9719	0.9702
		ii	0.9848	0.9801	0.9809

Figures

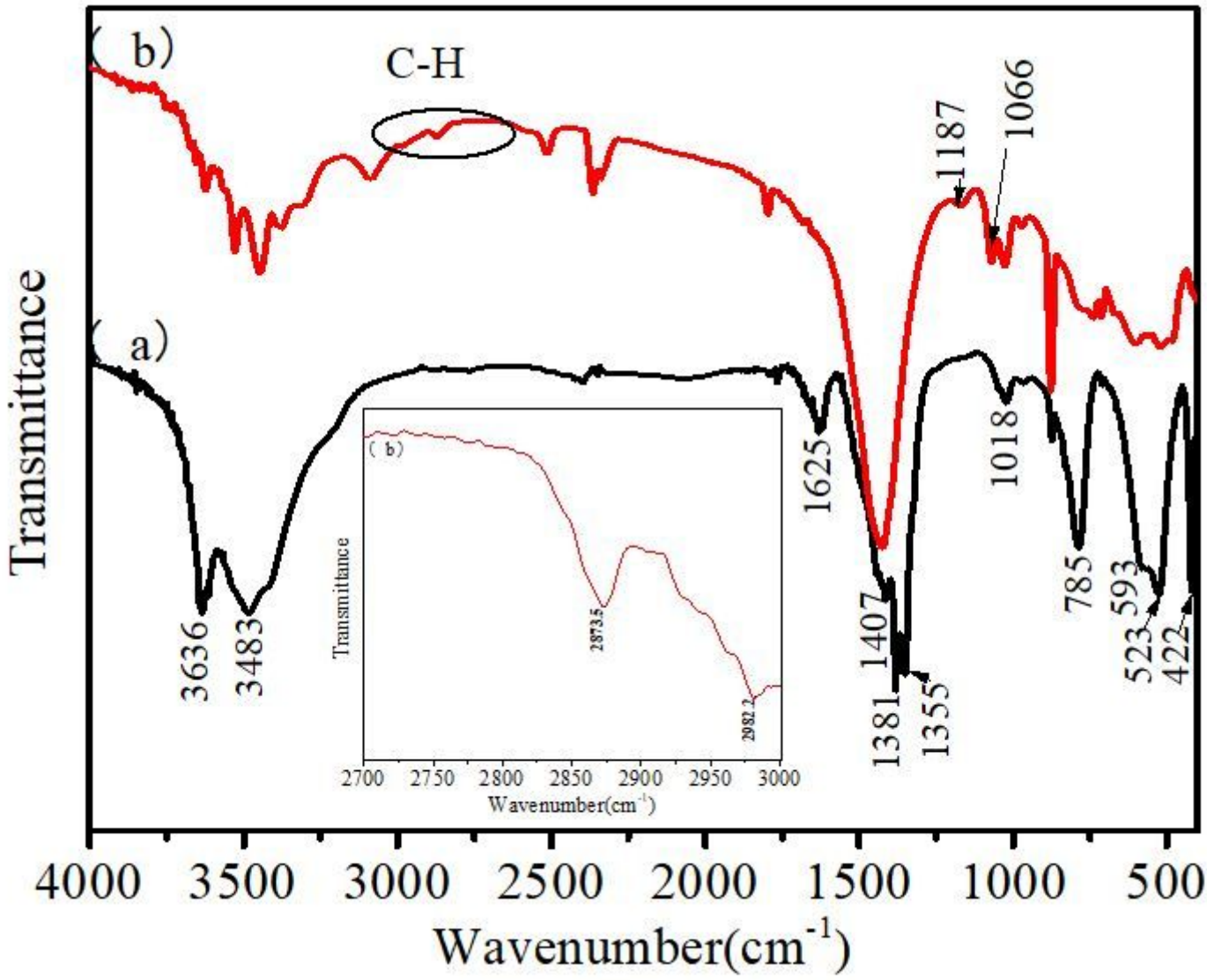

Figure 1

FT-IR spectra of CaAl-LDHs (a) and SDBS-CaAl-LDHs (b)

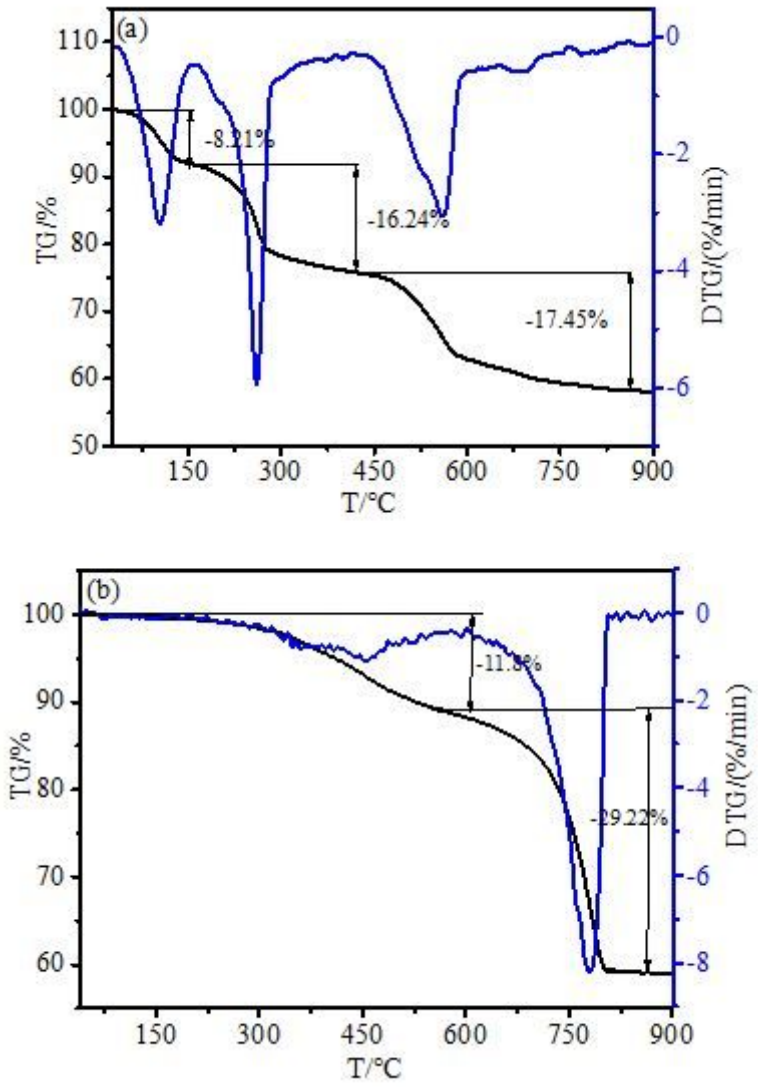

Figure 2

TG and DTG curves of CaAl-LDHs (a) and SDBS-CaAl-LDHs (b)

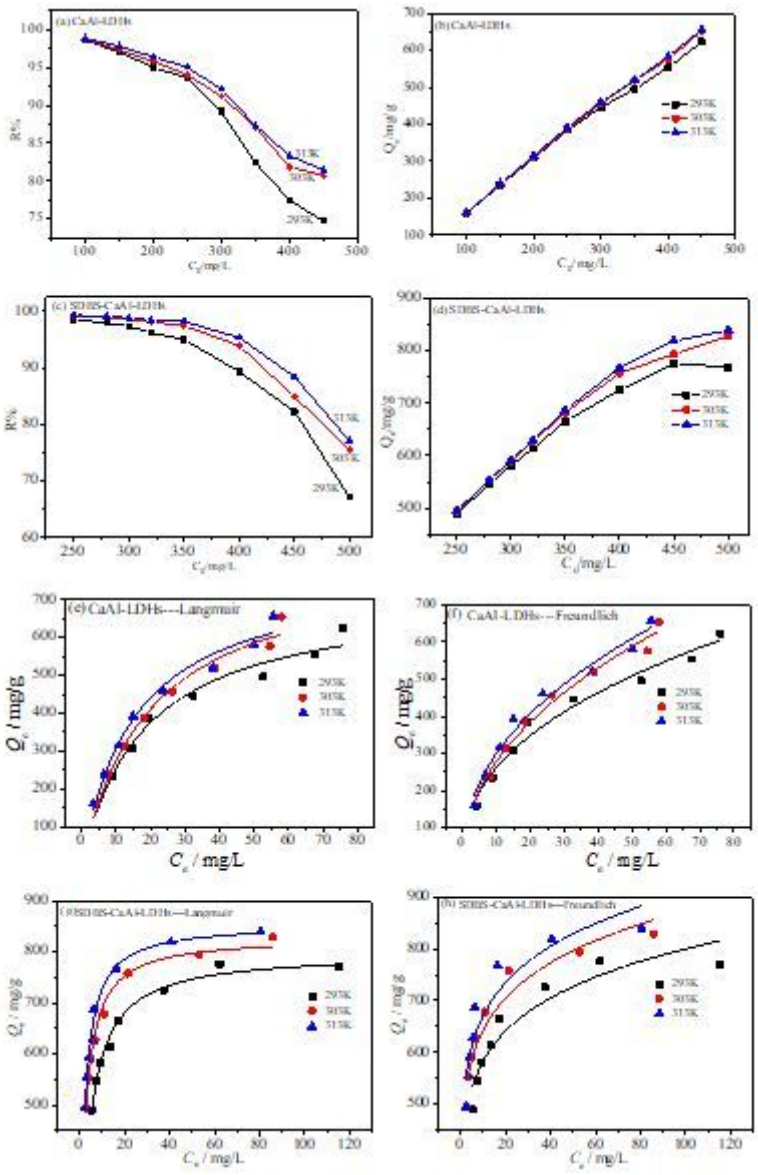

Figure 3

Effect of initial concentration on the adsorption of Pb2+ by CaAl-LDHs (a,b) and SDBS-CaAl-LDHs (c,d) and their adsorption isotherms (e~h); (adsorbent dosage for CaAl-LDHs and SDBS-CaAl-LDHs 0.06 and 0.05 g)

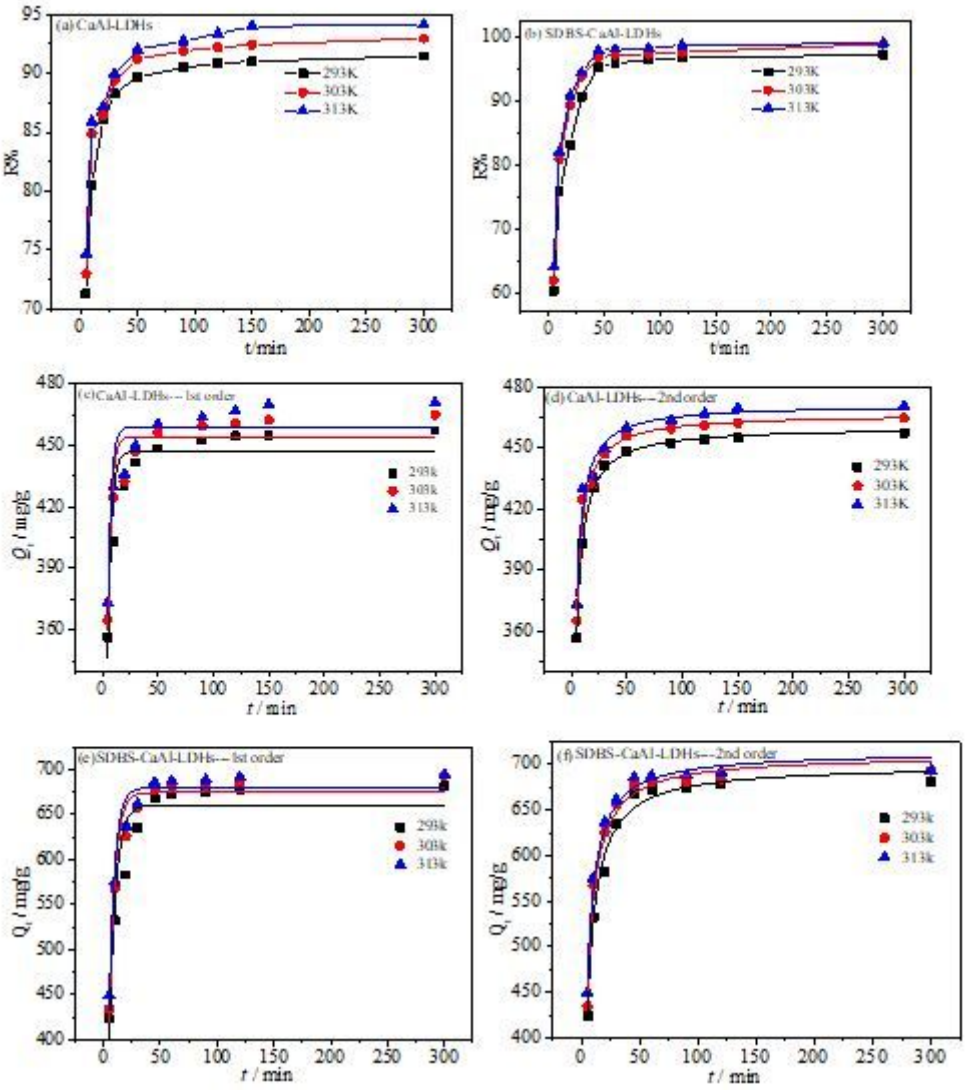

Figure 4

Effect of contact time on the adsorption of Pb2+ by CaAl-LDHs (a) and SDBS-CaAl-LDHs (b) and their adsorption kinetics (c~f) (Conditions: C0 = 300 mg L-1 , m = 0.06 g for CaAl-LDHs; C0 = 350 mg L-1 , m = 0.05 g for SDBS-CaAl-LDHs)

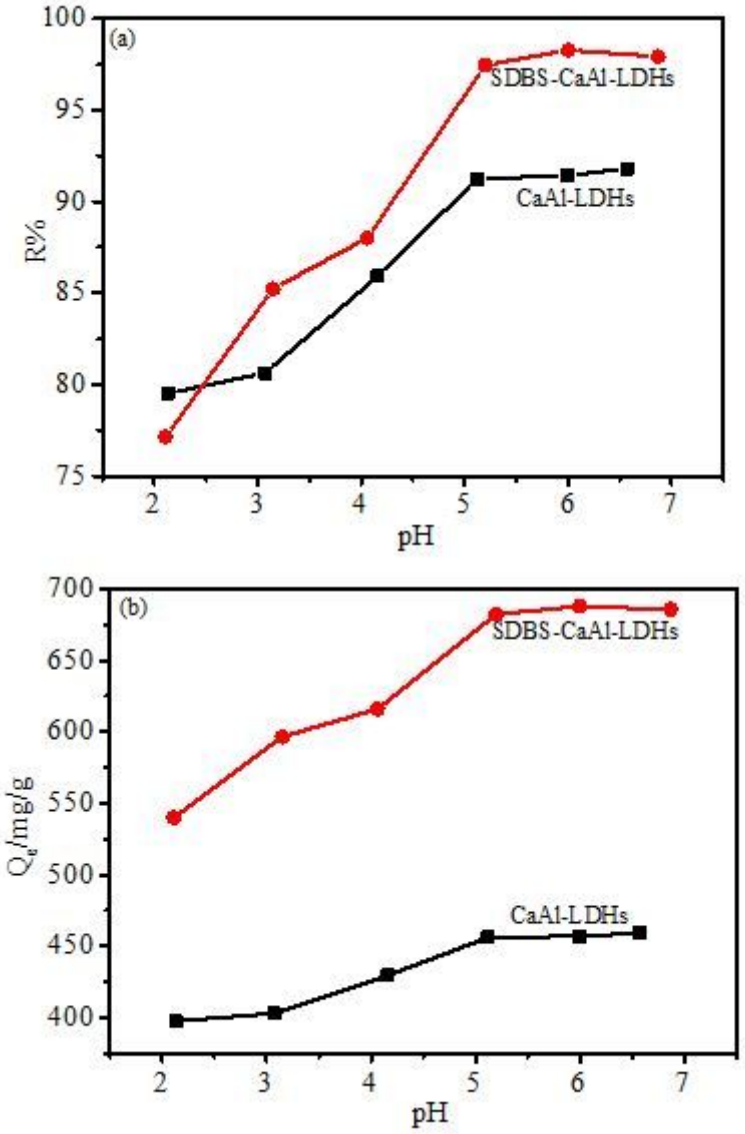

Figure 5

Effect of pH on the adsorption of Pb2+ by CaAl-LDHs and SDBS-CaAl-LDHs (Conditions: C0 = 300 mg L-1 , m = 0.06 g for CaAl-LDHs; C0 = 350 mg L-1 , m = 0.05 g for SDBS-CaAl-LDHs)

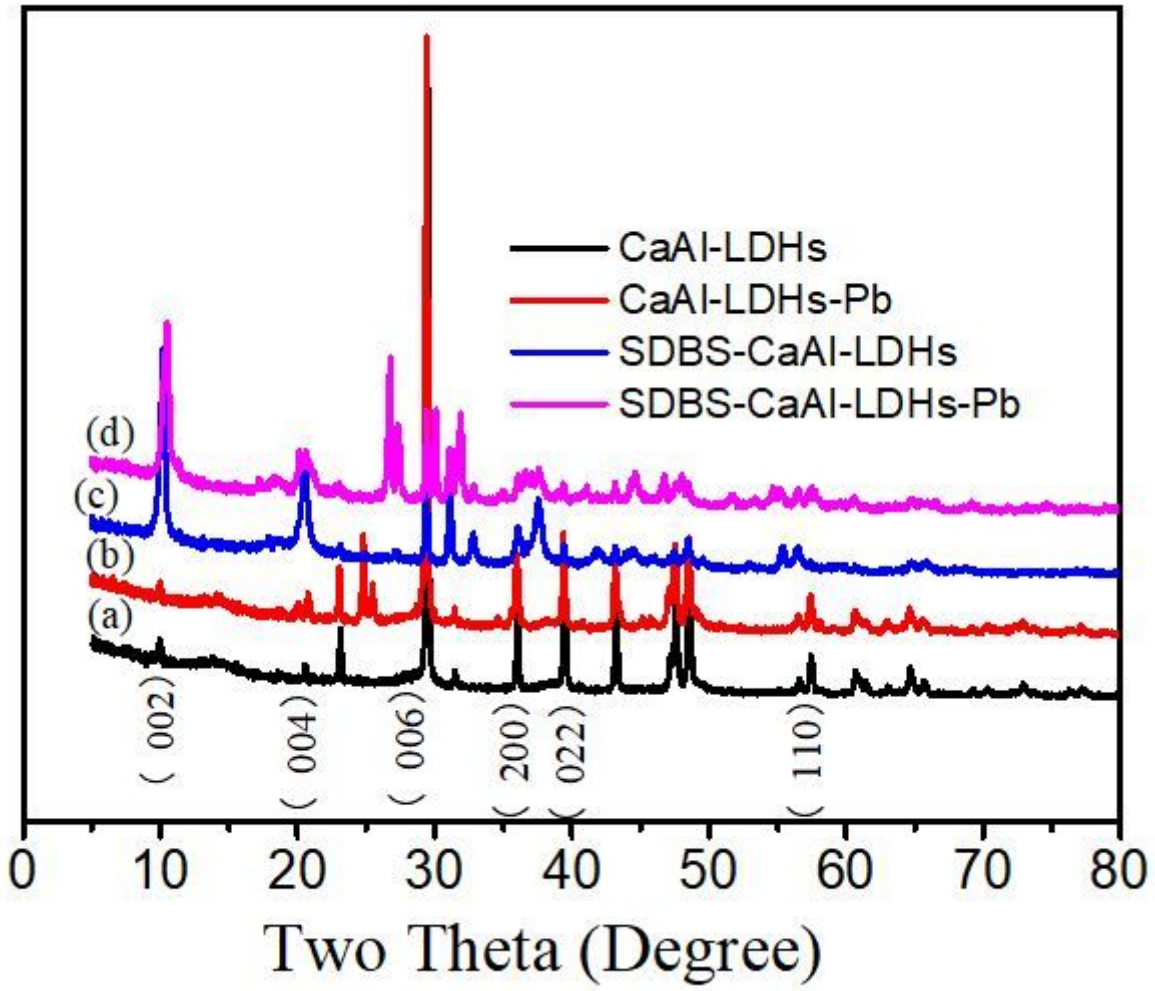

Figure 6

XRD patterns of adsorbents before and after lead ions adsorption

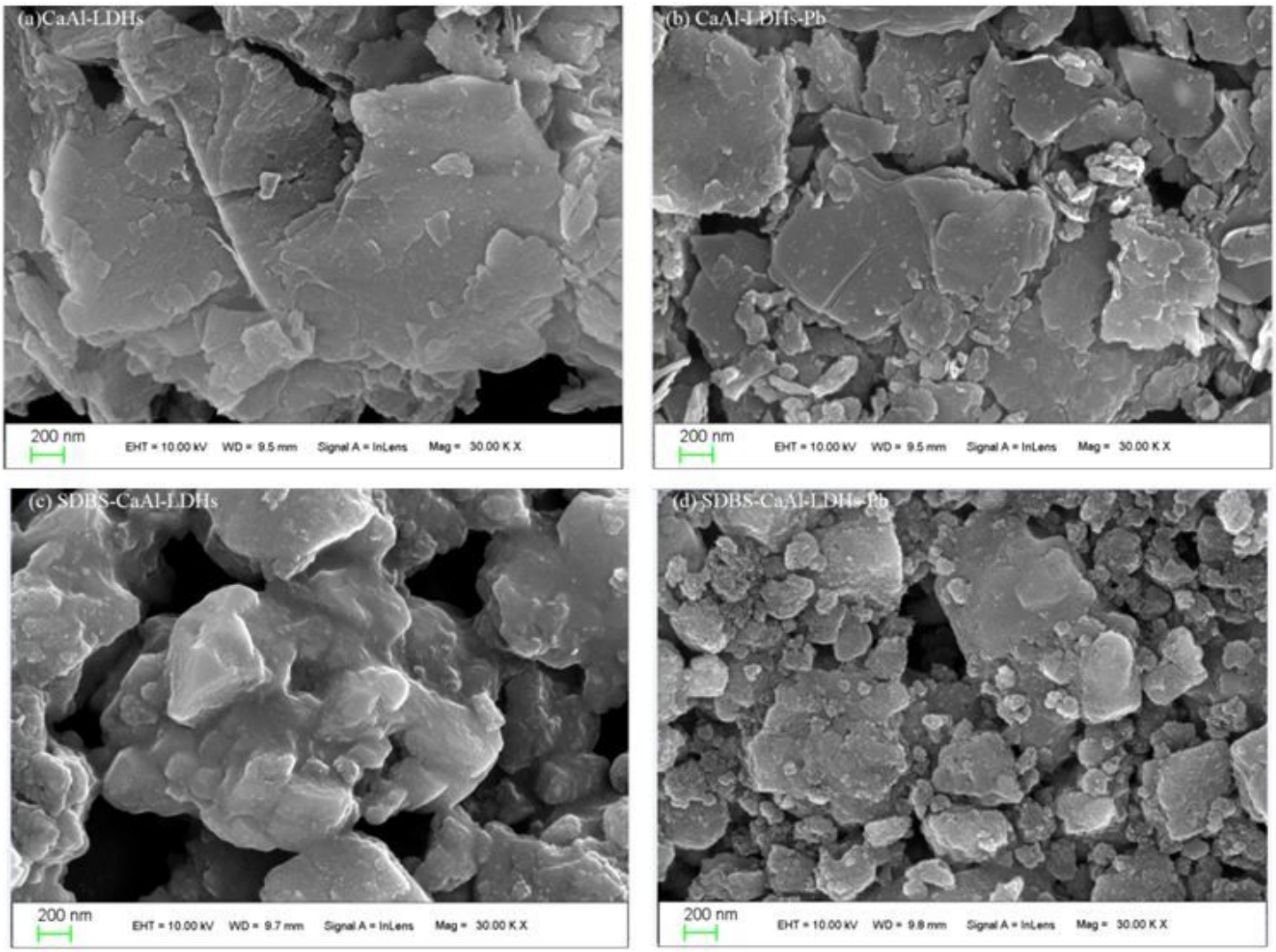

Figure 7

SEM images of adsorbents before and after lead ions adsorption

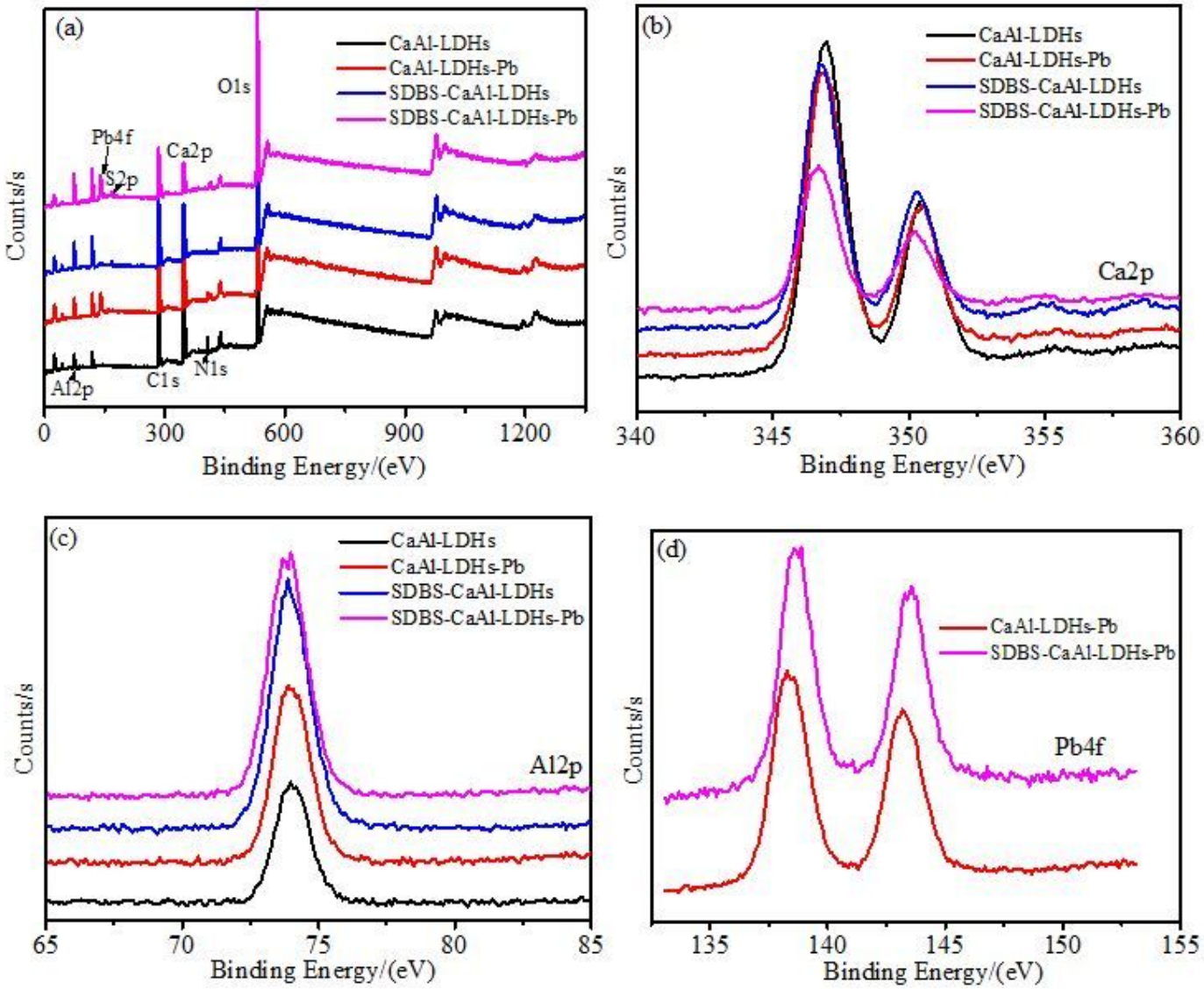

Figure 8

XPS spectra of CaAl-LDHs and SDBS-CaAl-LDHs before and after lead ions adsorption: (a) broad scan spectrum, (b) Ca 2p, (c) Al 2p, (d) Pb 4f, respectively

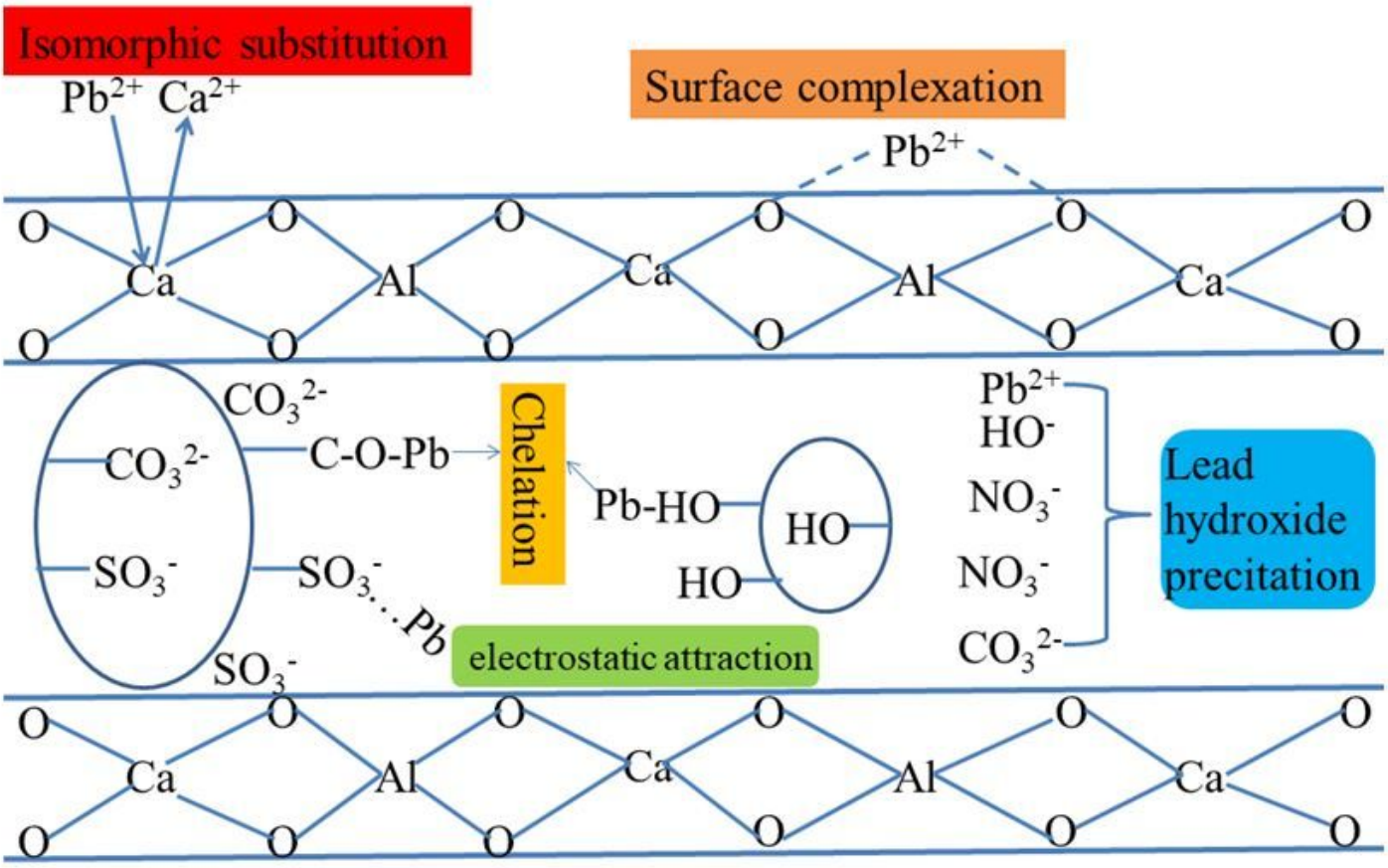

Figure 9

Propsed schematic illustration of lead ions sorption mechanisms on SDBS-CaAl-LDHs